Mushy Regions in Negative Squeeze Films

J.R. Ockendon and S.D. Howison,
Mathematical Institute, Oxford University,
24-29 St Giles, Oxford, OX1 3LB,

A.A. Lacey,
Department of Mathematics, Heriot–Watt University,
Riccarton, Edinburgh, EH14 4AS.

April 10, 2006

Abstract

An elegant experiment described in [13] suggests a novel free boundary model for the evolution of a mushy region in a negative squeeze film. The mushy region nucleates when the plates enclosing the film are pulled apart sufficiently rapidly for the pressure to drop to a critical value at some point of the film. On the basis of an earlier one-dimensional analysis, a complementarity model is proposed for quite general mush evolutions and a regularisation of this model is studied analytically and numerically.

1 Introduction

The phenomenon of cavitation is well known in the classical lubrication theory of bearings. It typically occurs when the lubricant enters a region in which the film thickness increases, with a concomitant decrease in pressure, and it leads to a variety of free boundary models [4, 7, 8, 10, 17]. It also occurs in 'negative squeeze films', in which the faces of a squeeze-film bearing are moved apart from each other. The situation in which an *isolated* fluid region surrounded by air at constant pressure contracts under the action of negative squeezing is discussed in [20, 21] However, although this configuration leads to an unstable free boundary model, it does not seem to be possible to regularise this model by the introduction of a mushy region, as was done for a class of Stefan problems with volumetric heating in [2, 16]. Nevertheless, there is a possibility of introducing a mushy region adjacent to a contracting liquid region in a negative squeeze film bearing that is initially *full* of liquid and immersed in a bath. The cavitation that initiates this mushy region was reported in the beautiful experiments of [13, 19].

Using a circular negative squeeze film bearing with parallel faces, immersed in a reservoir of fluid, [13, 19] found the patterns shown schematically in Fig. 1. The bearing remained full of liquid until a time t_i at which unstable cavitation was initiated at some nucleation point. At subsequent times, further unstable nucleation took place, each component of the cavity adopting a somewhat dendritic structure while the ensemble of cavities, or 'mushy region', had a reasonably well-defined boundary, shown dashed in Fig. 1. Then, at time t^*, the mushy region boundary stopped advancing and became more coherent, before contracting again until the film became full of liquid again at the extinction time $t = t_e$.
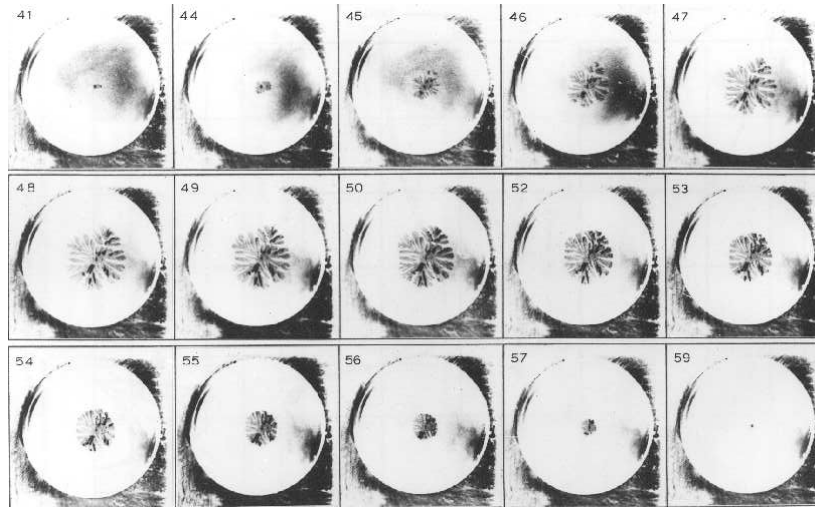
Figure 1: Experimental visualisation of cavitation, photograph courtesy of Prof J. Booker. The numbers are frame numbers; mush initiation at time t_i (frame 41) is followed by growth to turn-round at t^* (48/49), and contraction to extinction at t_e (59).

This phenomenon is of practical importance; it is involved in noise and wear in piston-pin bearings, for example, and has been described more fully, together with a theoretical explanation, in [5]. There a model is proposed in which the individual components of the cavitation region are ignored, yet the boundary of this region emerges from a numerical solution of Reynolds' equation for a compressible lubricant whose density is piecewise constant as a function of pressure, with a step-function increase at the cavitation (vapour) pressure. This solution was obtained by adapting a finite element cavitation code described in [14]. More recently [18] has given a novel free boundary formulation for the mushy region boundary, which we describe below, and which is explicitly solvable in one space dimension (or when there is radial symmetry). The explicit solution is used to validate the output of the finite element code of [6].

In company with these authors, we will neglect the intricacies involved in following individual components of the mushy region; this philosophy is explained in more detail in [15]. However, even with this simplification, the stability and monotonicity of the mushy region boundary pose interesting mathematical challenges. Hence, in this paper we begin in §2 by first recalling the model of [18], and formulating it as a two-dimensional free boundary problem. Then, in §3, we point out the relationship between this free boundary model and that of traditional Hele-Shaw flow between *fixed* parallel plates. We can thus use information about Hele-Shaw free boundary flows to make some observations about time-reversibility and then, in §4, to describe the asymptotics of mush nucleation and extinction. Then, in §5, we propose a regularisation of the model of §2 which provides the basis for a more systematic discussion of the mathematical properties of the solution and for the numerical experiments of §5.4.

2   A free boundary model

Suppose a negative squeeze film occupies the gap $0 < z < h(x, y, t)$ where (x, y) lies in some domain D (a circle in Fig. 1), and $\partial h / \partial t \geq 0$. Assuming the film to be full of lubricant, so that

the liquid fraction $\theta = 1$, Reynolds' equation for the dimensionless pressure p is

$$\nabla \cdot \left(\frac{h^3}{12} \nabla p \right) = \frac{\partial h}{\partial t}, \tag{2.1}$$

and p takes its ambient value, say

$$p = 1, \tag{2.2}$$

on ∂D; this is a simple model for the case in which the film is surrounded by a large reservoir of fluid. (We retain the factor 12 in (2.1) to make the reversion to dimensional variables more transparent.)

In the absence of any externally imposed nucleation mechanism, (2.1) implies that p first falls to the cavitation pressure, which we take to be zero without loss of generality, at some positive time t_i; we assume that $\partial h/\partial t = 0$ at $t = 0$ so that it is guaranteed that cavitation does not occur immediately, and we also assume that h increases sufficiently fast so that it does so eventually. The model of [18] proposes that thereafter there is a mushy region $\mathcal{M}(t)$ in which $p \equiv 0$ and the liquid fraction satisfies $0 < \theta < 1$; the remainder of D is the liquid region $\mathcal{L}(t)$ and the interface between $\mathcal{M}$ and $\mathcal{L}$ is denoted by $\Gamma(t)$.

In $\mathcal{M}$, there is no bulk flow of liquid, so that

$$\frac{\partial}{\partial t}(\theta h) = 0. \tag{2.3}$$

The all-important conditions on $\Gamma(t)$ have different implications depending on whether $\mathcal{M}(t)$ is expanding or contracting. In either case, we have

$$p = 0 \qquad \text{on} \quad \Gamma(t), \tag{2.4}$$

and we can also write down a mass balance in the form

$$-\frac{h^3}{12} \frac{\partial p}{\partial n} = h(1 - \theta)V_n; \tag{2.5}$$

here V_n is the velocity of the mush boundary directed inwards, towards the mush, and $\partial/\partial n$ is the normal derivative into $\mathcal{M}(t)$ (the reason for taking the inward normal to $\mathcal{M}(t)$ will become clear in the next section).

When $\mathcal{M}(t)$ expands, we have $V_n < 0$ and, because $p \geq 0$ in $\mathcal{L}(t)$, $\partial p/\partial n \leq 0$. Hence, from (2.5), we must have $\theta = 1$ on $\Gamma(t)$ and so the free boundary conditions are

$$p = 0, \quad \frac{\partial p}{\partial n} = 0 \qquad \text{on} \quad \Gamma(t). \tag{2.6}$$

When $\mathcal{M}$ contracts, on the other hand, the free boundary conditions are simply (2.4) and (2.5); however, the lubricant outside $\mathcal{M}$ is advancing into a mush in which $\theta < 1$ and θ is no longer continuous at the boundary.

The equations (2.1)–(2.5), together with the initial conditions and boundary conditions on ∂D, comprise the classical free boundary model of [18]. It is only at all easy to study its mathematical properties in cases of one-dimensional or radially-symmetric flow. The simplest one-dimensional case is when the given separation h is spatially constant and monotone increasing with $\dot{h}(0) = 0$ ($\dot{} = d/dt$). Then direct integration of (2.1) gives that for $t < t_i$, in the liquid

$$p(x,t) = 1 - \frac{6\dot{h}}{h^3}\left(1 - x^2\right) \tag{2.7}$$

3

where t_i, the time at which $p(0,t)$ first vanishes, is found from $6\dot{h}(t_i) = h^3(t_i)$. Thereafter, for $t_i < t < t^*$, the pressure, now denoted $p^+(x,t)$, and mushy region boundary $x = s^+(t)$ are given by

$$p^+ = \frac{6\dot{h}}{h^3}(x - s^+)^2, \qquad \text{where, from (2.2),} \quad s^+ = 1 - \sqrt{\frac{h^3}{6\dot{h}}}. \qquad (2.8)$$

In the mush, $\theta(x,t)h(t)$ is constant in t and equal to 1 times the value of $h(\tau(x))$ at the time

$$\tau(x) = (s^+)^{-1}(x) \qquad (2.9)$$

at which the advancing mush boundary reaches the point x; thus

$$\theta(x,t)h(t) = h(\tau(x)). \qquad (2.10)$$

The maximum extent of the mush is $s^+(t^*)$, where t^* is the time at which $d/dt\,(\dot{h}/h^3)$ first vanishes, so that $h(t^*)\ddot{h}(t^*) = 3\dot{h}^2(t^*)$.

Next, for $t > t^*$, writing the receding mush boundary as $x = s^-(t)$ and the pressure as $p^-(x,t)$,

$$p^- = \frac{6\dot{h}}{h^3}(x - s^-)^2 + A(t)(x - s^-) \qquad (2.11)$$

where from (2.2), (2.5)

$$\frac{6\dot{h}}{h^2}(1 - s^-)^2 + A(1 - s^-) = 1, \qquad \frac{-h^3}{12}A = h(1 - \theta)\dot{s}^-; \qquad$$

equation (2.10) still applies in the mush and and

$$s^+(\tau) = s^-(t). \qquad (2.12)$$

An explicit solution of this type is given in [18].

A reformulation of the classical model that may lead to further theoretical understanding in more general situations is the complementarity problem

$$\frac{\partial(\theta h)}{\partial t} + \nabla \cdot \left(\theta h \left(-\frac{h^2}{12}\nabla p\right)\right) = 0 \ \text{ in } \ D \qquad (2.13)$$

(there is a θ in the second term because this is, in general, the 'density'), with

$$p(1 - \theta) = 0 \qquad (2.14)$$

and

$$p \geq 0, \qquad 0 \leq \theta \leq 1, \qquad (2.15)$$

and with

$$\theta = 1 \quad \text{at} \ \ t = 0, \qquad (2.16)$$

$$p = 1 \quad \text{on} \ \ \partial D, \, t > 0. \qquad (2.17)$$

The model (2.13)–(2.15) has been proposed in [8] and is the basis for the regularised weak formulation that is studied in [4, 3]. We consider a different mathematical regularisation of this statement in §5, but first we look at some implications of the free boundary formulation.

4

3   Relationships with Hele-Shaw flows, reversibility

In this section we show that, in some circumstances, the free boundaries of an expanding mush and those of the same mush subsequently contracting generate the same family of curves, traced first in one direction then in the other. In this sense, the mush evolution is reversible. This result holds if h is a function of t alone, $h = h(t)$, and if the specified pressure on ∂D is also a function $p_0(t)$ of t alone; for more general $h(\mathbf{x}, t)$, it does not hold and indeed we may expect that for some h the mush boundary can be advancing in some places while it simultaneously recedes in others.

The reversibility is based on the observation that the squeeze film mush problem can be related to certain Hele-Shaw flows between fixed parallel plates and to their Baiocchi transforms, and from this we deduce that the normal velocity of a receding mush boundary is simply a certain function of t multiplied by the normal velocity of the same curve when it was an advancing mush boundary. Indeed, we shall present a 'universal' Hele-Shaw problem for the region D from whose solution we can calculate the mush evolution for *any* $h(t)$ and boundary pressure.

For simplicity, we only consider cases in which $p_0(t) = 1$ and the mush is nucleated at a single point at time t_i in the notation of section 1, expands monotonically until time t^* (we shall shortly see that this is while $\dot{h}(t)/h^3(t)$ is increasing), then contracts monotonically (while $\dot{h}(t)/h^3(t)$ is decreasing) until it disappears. Evidently this scenario requires that $\dot{h}(t)/h^3(t)$ has only one turning point. We say more about the local behaviour when the mush nucleates or vanishes in the next section.

The liquid while the mush is expanding.   We begin with the problem for the expanding mush, for times $t_i < t < t^*$. During this phase, the pressure in the liquid region $\mathcal{L}$, which we denote by $p^+(\mathbf{x}, t)$, satisfies

$$\nabla^2 p^+ = F(t) \qquad \text{in } \mathcal{L},$$

where $F(t) = 12\dot{h}(t)/h^3(t)$, with

$$p^+ = 1 \qquad \text{on } \partial D$$

and

$$p^+ = \frac{\partial p^+}{\partial n} = 0 \qquad \text{on } \Gamma^+.$$

Note that t only appears as a parameter in this problem. Indeed, setting $p^+(\mathbf{x}, t) = F(t)u^+(\mathbf{x}, t)$ we have

$$\nabla^2 u^+ = 1 \qquad \text{in } \mathcal{L}, \tag{3.1}$$

with

$$u^+ = \frac{1}{F(t)} = T(t), \quad \text{say} \tag{3.2}$$

on ∂D (the reason for this notation will become apparent shortly) and

$$u^+ = \frac{\partial u^+}{\partial n} = 0 \qquad \text{on } \Gamma^+. \tag{3.3}$$

We now recall that if a function $u^+(\mathbf{x}, t)$ satisfies (3.1), (3.3), then its time-derivative $v^+(\mathbf{x}, t)$ can be interpreted as the pressure in a standard Hele-Shaw free boundary problem in the region

$\mathcal{L}(t)$ with the normal to $\Gamma(t)$ taken outwards, into $\mathcal{M}(t)$ [10]. In fact, u^+ is the Baiocchi transform of v^+ [9], and the two are related by

$$v^+(\mathbf{x}, t) = \frac{\partial u^+(\mathbf{x}, t)}{\partial t}, \qquad u^+(\mathbf{x}, t) = \int_{\omega^+(\mathbf{x})}^{t} v^+(\mathbf{x}, \tau) \, d\tau,$$

where Γ^+ is $t = \omega^+(\mathbf{x})$. Furthermore, if u^+ additionally satisfies the constraint $u^+ \geq 0$, which is here enforced by our cavitation condition, then even if the corresponding Hele-Shaw problem has a receding free boundary (as it does when the mush is expanding), it does not suffer terminal blow-up via cusps or other singularities in its free boundary. Instead, if necessary, it avoids this fate by nucleating new components of its free boundary [12].

The problem for v^+ is

$$\nabla^2 v^+ = 0 \qquad \text{in } \mathcal{L},$$

with

$$v^+ = \dot{T}(t) \quad \text{on } \partial D$$

and

$$v^+ = 0, \quad \frac{\partial v^+}{\partial n} = -V_n \qquad \text{on } \Gamma^+.$$

It is now clear that the mush expands when the boundary 'pressure' $\dot{T}(t)$ for the corresponding Hele-Shaw problem is negative, that is when $F(t)$ is increasing, as stated above. We also see that the whole of Γ 'turns round' at the same time t^*, found from $\dot{T}(t^*) = 0$.

We can in fact transform the problem for v^+ to remove the time-dependence altogether. We interpret T as a fictitious time, noting that $\dot{T} < 0$ during the expansion period. We then set $v^+ = \dot{T}\hat{v}$, to find that $\hat{v}$ satisfies

$$\nabla^2 \hat{v} = 0 \qquad \text{in } \mathcal{L},$$

with

$$\hat{v} = 1 \qquad \text{on } \partial D$$

and

$$\hat{v} = 0, \quad \frac{\partial \hat{v}}{\partial n} = -\hat{V}_n \qquad \text{on } \hat{\Gamma},$$

where $\hat{V}_n = V_n/\dot{T}$ is the normal velocity of the free boundary $\hat{\Gamma}$ for this problem using the new 'time' T. The 'pressure' for this canonical Hele-Shaw flow is related to u^+ above by $\hat{v} = \partial u^+/\partial T$. As we shall see, the variable $\hat{v}$ is central to our analysis of the contracting mush.

As was apparent from (3.1)–(3.3), we have been able to reformulate the problem without reference to $F(t)$. It follows that with the correct 'initial' condition for $\hat{v}$, the solution of this one problem will tell us the solution to the squeeze film problem for *any* F. Different separation rates for the plates simply correspond to Γ^+ traversing different subsets of the same family of curves at different rates, but in each case for times such that $F(t)$ is increasing. The turn-around curve, at which $\dot{F} = 0$, is a 'high-water mark' determined solely by the maximum value of F. In particular, if $F \to \infty$ monotonically, $\Gamma^+ \to \partial D$.

We could, of course, solve the receding Hele-Shaw problem for $\hat{v}$ with a free boundary that starts as a point at the nucleation point; however, this first requires us to locate this point. Alternatively, we can note that the Hele-Shaw problem is time-reversible, and use the observation that if $F \to \infty$, $\Gamma^+ \to \partial D$. We can therefore generate the required set of curves by solving an *expanding* Hele-Shaw problem for $\hat{v}$ with 'initial' free boundary equal to ∂D. This

will give a sequence of curves $\hat{\Gamma}(T)$, with eventual extinction at a point (assumed unique) as D is filled up. Note that this procedure locates the nucleation point automatically. The sequence of free boundaries for the expanding mush is then simply the set of curves $\hat{\Gamma}(T)$, taken in reverse order starting from the nucleation point at $t = t_i$, and continuing with t and T related by (3.2) until time t^*.

The mush. Whether the mush region $\mathcal{M}$ is expanding or contracting, the liquid fraction inside it satisfies

$$\frac{\partial}{\partial t}(\theta h) = 0, \quad \text{with} \quad \theta = 1 \quad \text{on } \Gamma.$$

We therefore have

$$\theta(\mathbf{x}, t) = h\left(\omega^+(\mathbf{x})\right) / h(t) \tag{3.4}$$

for times $\omega^+(\mathbf{x}) < t < \omega^-(\mathbf{x})$, where $\omega^-(\mathbf{x})$ is the time at which the receding mush boundary reaches $\mathbf{x}$.

The liquid while the mush is contracting. For times $t^* < t < t_e$, during which the mush is contracting to extinction at $t = t_e$, the liquid pressure $p^-(\mathbf{x}, t)$ satisfies

$$\nabla^2 p^- = F(t) \qquad \text{in } \mathcal{L},$$

with

$$p^- = 1 \qquad \text{on } \partial D$$

and

$$p^- = 0, \quad -\frac{h^2}{12}\frac{\partial p^-}{\partial n} = (1 - \theta)V_n \qquad \text{on } \Gamma^-(t). \tag{3.5}$$

This is evidently closely related to a Hele-Shaw problem such as that for v^+ described above. The crucial observations that point to reversibility are

- If $\Gamma^-(t)$ coincides with a curve $\Gamma^+(\tau(t))$ for some $\tau(t)$, then by (3.4), $\theta(\mathbf{x}, t)$ is constant along $\Gamma^-(t)$. The factor $(1 - \theta)$ in (3.5) is thus independent of position on Γ^- and, for that t, the problem for p^- has aspects of both a standard Hele-Shaw problem and its Baiocchi transform; we remember that we can scale out time-dependence in the coefficients of a Hele-Shaw problem.

- We know that there is a Hele-Shaw problem, with spatially-independent 'pressure' on ∂D, whose free boundaries are Γ^+.

These considerations suggest that we try the effect of writing $\Gamma^-(t) = \hat{\Gamma}(T) = \Gamma^+(\tau(t))$, where $\tau(t)$ is the time at which the advancing mush boundary crossed the curve Γ^-, so that $\omega^+(\mathbf{x}) = \tau(t)$. Correspondingly, we try to find a function $A(t)$ such that

$$p^-(\mathbf{x}, t) = F(t)u^+(\mathbf{x}, \tau(t)) + A(t)\hat{v}(\mathbf{x}, \tau(t)),$$

where u^+ and $\hat{v}$ are as above. We satisfy the condition $p^- = 1$ on ∂D by taking

$$A(t) = 1 - F(t)T^-(t).$$

It only remains to satisfy the kinematic condition

$$-\frac{h^2}{12}\frac{\partial p^-}{\partial n} = (1 - \theta)V_n.$$

As $\partial \hat{v} / \partial n = -\hat{V}_n$, we have

$$-\frac{h^2(t)}{12} (1 - F(t)T(\tau(t))) \hat{V}_n = -(1 - \theta) V_n(t).$$

However, as $V_n / \hat{V}_n = \dot{T}(t)$ and $\theta = h(\tau(t)) / h(t)$, we can verify that $\Gamma^-(t)$ is indeed $\Gamma^+(\tau(t))$ as long as we ensure that T satisfies

$$\dot{T}(t) = \frac{h^2 \left(1 - F(t)T(\tau(t)) \right)}{12 \left(1 - h(\tau(t))/h(t) \right)} \tag{3.6}$$

(in which $T(\tau(t))$ is known from the solution of the advancing phase) and the solution of this differential equation for $T(t)$ gives the evolution of the contracting mush boundary. We have therefore given an explicit construction for the contracting phase, demonstrating the reversibility claimed above.

4 Mush initiation, turn-round and extinction

We now consider the local behaviour near the times t_i, t^* and t_e, at which the mush nucleates, turns round and vanishes respectively. To avoid unnecessary complications, we continue to assume that h is independent of $\mathbf{x}$.

Mush initiation/extinction. From the previous section, both the local behaviour when $\mathcal{M}$ starts to form at $t = t_i$, and its final contraction to (typically) a point, are given by the expansion (or contraction) of a bubble in Hele-Shaw flow. Now the asymptotic contraction of a bubble in the whole plane has been considered by [11]. There, it was shown for a bubble with a single extinction point that the final point is at the minimum of a function which satisfies Poisson's equation in the initial bubble and is harmonic outside it. The asymptotic shape of the bubble is elliptical and related to the local level sets of the function just mentioned. We also note the survey of [1], in which the corresponding nucleation/extinction problem for the Stefan problem is treated in detail.

As our reversibility analysis shows that the initiation and extinction limits are essentially identical, we only look at the initial growth phase, t near t_i. We restrict our attention to the generic case where:

(a)
$$F(t) = 12\dot{h}(t)/h^3(t) \quad \text{satisfies} \quad F(t_i) = F_i > 0, \ \dot{F}(t_i) = \dot{F}_i > 0$$

(it is quite easy to generalise, to allow for other cases of F increasing but with $\dot{F}(t_i) = 0$).

(b) In line with the discussion above, the mush $\mathcal{M}$ forms at a single point. This means that if w is defined to be the solution to

$$\nabla^2 w = 1 \quad \text{in } D, \quad w = 0 \quad \text{on } \partial D, \tag{4.1}$$

there is just one point $\mathbf{x}_0$ at which

$$w(\mathbf{x}_0) = w_M = \min_{\mathbf{X} \in D} w(\mathbf{x}).$$

We then have that $p = 1 + F(t)w(\mathbf{x})$ for $t < t_i$, and $\mathcal{M}$ forms at $\mathbf{x}_0$ at the time t_i such that $F_i = -1/w_M$. We may assume that $\mathbf{x}_0 = \mathbf{0}$.

(c) We assume that the local behaviour of w near $\mathbf{x} = \mathbf{0}$ is given by

$$w \sim -1/F_i + \frac{1}{2}(ax^2 + (1-a)y^2) \quad \text{for} \quad (x, y) \to \mathbf{0} \quad \text{with} \quad 0 < a < 1. \tag{4.2}$$

Now for $0 < t - t_i \ll 1$, $\mathcal{M}$ will be of some size $\delta(t) \ll 1$, so we write $\mathcal{M} = \delta\widetilde{\mathcal{M}}$ or $\mathcal{M} = \{\mathbf{x} : \mathbf{x}/\delta \in \widetilde{\mathcal{M}}\}$. Of course, there is some indeterminacy here because δ, which is to be determined, can be multiplied by any $O(1)$ constant and $\widetilde{\mathcal{M}}$ correspondingly shrunk. In any case there is some C, fixed by $\widetilde{\mathcal{M}}$ and independent of δ, such that away from $\mathbf{0}$

$$p \sim 1 + (F_i + \dot{F}_i(t - t_i))w - C\delta^2(\ln|\mathbf{x}| + W),$$

where

$$\nabla^2 W = 0 \quad \text{in } D \quad \text{with} \quad W = -\ln|\mathbf{x}| \quad \text{on } \partial D.$$

If we take $\mathbf{x} \to \mathbf{0}$ in this outer solution, we find that

$$p \sim -\frac{\dot{F}_i}{F_i}(t - t_i) + \frac{F_i}{2}(ax^2 + (1-a)y^2) - C\delta^2 \ln|\mathbf{x}| - C\delta^2 W(\mathbf{0}), \tag{4.3}$$

and an inner solution, valid for $|\mathbf{x}| = O(\delta)$, should match with this. On writing

$$\mathbf{x} = \delta\tilde{\mathbf{x}}, \quad p = \frac{\delta^2 F_i}{4}(|\tilde{\mathbf{x}}|^2 - 2\tilde{p}),$$

we see that the new "pressure" $\tilde{p}$ satisfies the leading-order problem

$$\nabla^2 \tilde{p} = 0 \quad \text{outside } \widetilde{\mathcal{M}}, \tag{4.4}$$

$$\tag{4.5}$$

$$\tilde{p} = \frac{1}{2}|\mathbf{x}|^2 \quad \text{and} \quad \frac{\partial \tilde{p}}{\partial n} = \frac{1}{2}\frac{\partial}{\partial n}|\tilde{\mathbf{x}}|^2 \quad \text{on } \tilde{\Gamma} = \partial\widetilde{\mathcal{M}}. \tag{4.6}$$

In order to match with (4.3),

$$\tilde{p} \sim \left(\frac{1}{2} - a\right)\tilde{x}^2 + \left(a - \frac{1}{2}\right)\tilde{y}^2 + \frac{2C}{F_i}\ln|\tilde{\mathbf{x}}| + \frac{2}{F_i}\left(\frac{\dot{F}_i(t - t_i)}{F_i\delta^2} + C\ln\delta + CW(\mathbf{0})\right) \tag{4.7}$$

as $|\tilde{\mathbf{x}}| \to \infty$.

Now the equation and boundary conditions (4.4), (4.6) mean that

$$g(z) = \frac{\partial \tilde{p}}{\partial \tilde{x}} - i\frac{\partial \tilde{p}}{\partial \tilde{y}}$$

is the Schwarz function (see [11]) for $\tilde{\Gamma}$: g is an analytic function of $\tilde{z} = \tilde{x} + i\tilde{y}$ and $\tilde{\Gamma}$ is given by $\bar{\tilde{z}} = \tilde{x} - i\tilde{y} = g(\tilde{z})$. The growth condition (4.7) gives

$$g \sim (1 - 2a)\tilde{z} + \frac{2C}{F_i\tilde{z}} + o\left(\frac{1}{\tilde{z}}\right) \quad \text{for } \tilde{z} \to \infty, \tag{4.8}$$

which suggests that $\tilde{\Gamma}$ is elliptical, as the ellipse $\tilde{x}^2/\alpha^2 + \tilde{y}^2/\beta^2 = 1$ has Schwarz function

$$g(\tilde{z}) = \frac{\left(\alpha^2 + \beta^2\right)\tilde{z} - 2\alpha\beta\sqrt{\tilde{z}^2 - \alpha^2 + \beta^2}}{\alpha^2 - \beta^2}$$

$$\sim \frac{(\alpha - \beta)\tilde{z}}{(\alpha + \beta)} + \frac{\alpha\beta}{\tilde{z}} \quad \text{for } \tilde{z} \to \infty. \tag{4.9}$$

9

If we compare (4.8) with (4.9), we see that

$$a = \frac{\beta}{\alpha + \beta}, \quad C = \frac{\alpha \beta F_i}{2}.$$

Moreover, for full matching between the inner and outer solutions we need

$$\frac{\dot{F}_i}{F_i}(t - t_i) \sim -C\delta^2 \ln \delta.$$

If we wish to remove the indeterminacy mentioned earlier we can fix, for example, $\alpha + \beta = 1$; in this case,

$$\alpha = 1 - a, \quad \beta = a, \quad C = \frac{F_i}{2}a(1-a) \quad \text{and} \quad \delta \sim \frac{2}{F_i}\sqrt{\frac{\dot{F}_i(t-t_i)}{a(1-a)|\ln(t-t_i)|}} \quad \text{for } t \downarrow t_i.$$

As mentioned above, the final contraction back to **0** is quite similar.

Turn-round. The other most interesting time is $t = t^*$, the turning time. To keep things relatively simple, a generic case is considered for which we assume that

$$\dot{F} > 0 \quad \text{for } t_i \leq t < t^*, \quad \dot{F}(t^*) = 0, \ \ddot{F}(t^*) < 0.$$

In this case,

$$F(t) \sim F^* - c(t - t^*)^2 \quad \text{for} \quad t \to t^* \quad \text{with} \quad F^* = F(t^*) > 0, \ c > 0.$$

Since $F = 12\dot{h}/h^3$, the corresponding local behaviour for $h(t)$ is

$$h \sim h^* + \frac{F^* h^{*3}}{12}(t - t^*) + \cdots \quad \text{for } t \to t^*, \tag{4.10}$$

where $h^* = h(t^*)$.

Now consider times such that $\Gamma(t)$ is close to $\Gamma(t^*) = \Gamma^*$. Taking a fixed point on Γ^*, we write S for the normal distance from this point to $\Gamma(t)$. We have that

$$\frac{dS}{dt} \sim -V_n.$$

Let us first examine times just before turn-round. We can calculate $-V_n$ by recalling from the previous section that it is the normal derivative of the function v^+ that satisfies

$$\nabla^2 v^+ = 0 \qquad \text{in } \mathcal{L},$$

with

$$v^+ = \dot{T}(t) = -\dot{F}/F^2 \quad \text{on } \partial D$$

and

$$v^+ = 0 \quad \text{on } \Gamma^+.$$

Since $\dot{F}/F^2 \sim 2c(t - t^*)/F^{*2}$ for t near t^*, we have that

$$\frac{dS}{dt} \sim -\frac{2c(t - t^*)}{F^{*2}}V_n^* \quad \text{for } t \uparrow t^*,$$

10

where V_n^*, the normal derivative on Γ^* of $-F^{*2}v^+(x,t^*)/2c(t-t^*)$, depends to lowest order on position but not t. It follows that for a point $\mathbf{x}$ just inside Γ^*,

$$S \sim \frac{c}{F^{*2}}(t-t^*)^2 V_n^* \quad \text{for } t \uparrow t^*.$$

We also have that $\omega(\mathbf{x})$, the time at which $\mathbf{x}$ is first crossed by Γ near Γ^*, is approximately given by

$$\omega(\mathbf{x}) \sim t^* - F^* \sqrt{\frac{S}{cV_n^*}},$$

using the same notation as above.

To analyse the times just after turn-round, we return to the pseudo-time T of the previous section. From the discussion above, we have

$$T \sim \frac{1}{F^*} + c(t-t^*)^2/F^{*2} + \cdots \quad \text{for } t \uparrow t^*.$$

Equivalently, the time $t = \tau(T) < t^*$, at which $\Gamma(t) = \Gamma_T$ satisfies

$$\tau \sim t^* - F^* \sqrt{\frac{T - 1/F^*}{c}} \quad \text{for } T \downarrow \frac{1}{F^*} \text{ (i.e. } t \downarrow t^*\text{).}$$

The term $\theta = 1 - h(\tau(T))/h(t)$ which appears in (3.4) is approximately

$$\frac{h^* - \left(F^* h^{*3}/12\right) F^* \sqrt{\frac{T-1/F^*}{c}}}{h^* + \left(6F^* h^{*3}/12\right)(t-t^*)} \sim \frac{h^{*2} F^*}{12} \left(F^* \sqrt{\frac{T-1/F^*}{c}} + (t-t^*)\right)$$

for $t \downarrow t^*$, $T \downarrow 1/F^*$. Also (3.6) gives

$$\dot{T} \sim \frac{[1 - (F^* - c(t-t^*)^2)T]}{F^* \left(F^* \sqrt{\frac{T-1/F^*}{c}} + (t-t^*)\right)}.$$

Hence, if we look for a local solution of the form $T \sim 1/F^* + \gamma(t-t^*)^2 + \cdots$, we have

$$2\gamma(t-t^*) \sim \frac{c(t-t^*)^2/F^* - F^*\gamma(t-t^*)^2}{F^* \left(F^* \sqrt{\frac{\gamma}{c}}(t-t^*) + (t-t^*)\right)},$$

and we find that γ must be given by

$$(2F^{*2}/\sqrt{c})\gamma^{3/2} + (3F^*)\gamma = c/F^*.$$

This is a cubic equation for $\gamma^{\frac{1}{2}}$ and clearly has a single real solution satisfying

$$0 < \gamma < c/F^{*2}.$$

It follows that as t increases from t^* the distance moved from Γ^* is again quadratic in time, specifically

$$s \sim \gamma V_n^* (t-t^*)^2 \quad \text{for } t \downarrow t^*,$$

where V_n^* is as above; however, the constant of proportionality is different from that just before t^*, being γV_n^*, not cV_n^*/F^{*2}.

We repeat that, for there to be a well-defined turning time, it is vital that h be restricted, such as $h = h(t)$, to avoid possibilities of $\mathcal{M}$ both expanding and partly contracting.

11

5 A regularised model

As an alternative to direct analysis of the free boundary formulation of §2, we now present a regularisation which sheds some further light on the properties discussed in §3, §4. In the spirit of the compressibility models of [7], [14], we simply replace (2.14) by

$$p(1 - \theta) = \epsilon,$$

where ϵ is a small positive number. Assuming that $\theta < 1$, this leads at once to the parabolic equation

$$\frac{\partial}{\partial t}(\theta h) = \epsilon \nabla \cdot \left(\frac{h^3 \theta}{12(1 - \theta)^2} \nabla \theta \right), \tag{5.1}$$

with

$$\theta = 1 - \epsilon \quad \text{on } \partial D \tag{5.2}$$

and with a suitable initial condition.

We now consider the asymptotic solution of (5.1) for the scenario described in the Introduction. We will only consider the case of one-dimensional flow with $h = h(t)$ as in §2, but our asymptotic decomposition applies to much more general flows. Even when the flow is not time-reversible, in particular when V_n is not of one sign on the free boundary, we may expect the analysis of turn-round given below to apply locally, near each point of Γ near the time of its furthest penetration into the liquid.

5.1 Expanding mush

For $t < t_i$, (5.1) is approximated by

$$\theta \sim 1, \qquad \frac{\partial h}{\partial t} = \frac{\partial}{\partial x}\left(\frac{h^3}{12} \frac{\partial p}{\partial x} \right),$$

leading to (2.7). For $t^* > t > t_i$, the lowest-order solution for the liquid and mush regions is still (2.8), (2.10). Now they are joined smoothly by a "mush boundary" which is described locally items of a coordinate $\xi = (x - Vt)/\nu$ where $V \ (> 0)$ is the locally frozen value of $\dot{s}(t)$ (thus, $V = -V_n$) and ν a small parameter to be determined. In this boundary layer, we also scale $\theta = 1 - \eta\varphi$, where η is also to be determined. To lowest order, (5.1) becomes

$$\frac{\partial h}{\partial t} + V \frac{h\eta}{\nu} \frac{\partial \varphi}{\partial \xi} = -\frac{\epsilon}{\eta \nu^2} \frac{h^3}{12} \frac{\partial}{\partial \xi}\left(\frac{1}{\varphi^2} \frac{\partial \varphi}{\partial \xi} \right). \tag{5.3}$$

Now, to match with (2.8), we need $\theta = 1 - \epsilon/p \sim 1 - O(\epsilon/\nu^2\xi^2)$ as $\xi \to +\infty$, and hence, since $\theta = 1 - \eta\varphi$, we must have $\eta = \epsilon/\nu^2$. Moreover, (2.10) gives that $\theta = 1 + O(\nu\epsilon)$ as we approach the boundary layer from the mush and matching outward from this layer as $\xi \to -\infty$ can only be achieved if $\nu = \eta$. Thus $\nu = \eta = \epsilon^{1/3}$, all the terms in (5.3) are in balance, and we obtain

$$-\frac{h^3}{12\varphi^2} \frac{\partial \varphi}{\partial \xi} = (\xi - \xi_0(t)) \frac{\partial h}{\partial t} + Vh\varphi \tag{5.4}$$

for some function $\xi_0(t)$ that can only be determined by higher-order matching. Now since $V > 0$, it is easy to see that

$$\varphi \sim \frac{2h^3}{\dot{h}} \frac{1}{\xi^2} \text{ as } \xi \to +\infty, \tag{5.5}$$

$$\varphi \sim -\frac{1}{Vh} \frac{\partial h}{\partial t} \xi \text{ as } \xi \to -\infty \tag{5.6}$$

as required by our outer solution in §2.

5.2 Contracting mush

Things are different for $t > t^*$, when $V < 0$. Then, from (2.5), we have no reason to rescale θ in the mush boundary, so $\eta = 1$ and we abandon our other relations between δ, ν and ϵ. The terms in (5.3) can only balance if $1/\nu = \epsilon/\nu^2$, i.e. $\nu = \epsilon$, and thus the mush boundary is now described by

$$-Vh\frac{\partial\theta}{\partial\xi} = \frac{h^3}{12}\frac{\partial}{\partial\xi}\left(\frac{\theta}{(1-\theta)^2}\frac{\partial\theta}{\partial\xi}\right)$$

which implies that

$$-V(\theta - \theta_0) = \frac{h^2\theta}{12(1-\theta)^2}\frac{\partial\theta}{\partial\xi} \tag{5.7}$$

where θ_0 is the value of θ as the mush boundary is approached from the mush region. Thus

$$\theta \sim \theta_0 + O(e^{-V(1-\theta_0)^2\xi/\theta_0}) \tag{5.8}$$

as $\xi \to -\infty$, and as $\xi \to +\infty$

$$\theta \sim 1 + \frac{h^2}{V(1-\theta_0)\xi}, \qquad p \sim -\frac{V(1-\theta_0)\xi}{h^2} \tag{5.9}$$

in accordance with (2.5).

5.3 Turn-round

This just leaves us with the "turnover region" near $t = t^*$, $s = s^* = s(t^*)$. We write $\theta = 1 - \eta^*\phi$, $t - t^* = \zeta^*\tau$ and $x - s^* = \nu^*\xi$, where η^*, ζ^* and ν^* are all to be determined in terms of ϵ. Anticipating that, as in the explicit solution (2.8)–(2.9), the boundary layer is centred around the parabolas

$$x - s^* \sim -k^-(t-t^*)^2, \qquad t < t^*$$
$$x - s^* \sim -k^+(t-t^*)^2, \qquad t > t^*,$$

where k^- and k^+ are constants, which as we saw in §4 need not necessarily be equal, we demand that $\nu^* = \zeta^{*2}$. Now the turnover region is distinguished by the fact that the second term in (5.3) represents 'convection' which is no longer via a wave travelling with speed V, but rather by an acceleration on the τ scale, i.e. $V \partial/\partial\xi$ becomes $-\partial/\partial\tau$. Hence, since the first term in (5.3) remains of $O(1)$ as $\epsilon \to 0$, a balance in this equation is only achieved when

$$1 = \frac{\eta^*\zeta^*}{\nu^*} = \frac{\epsilon}{\eta^*\nu^{*2}}.$$

We find $\nu^* = \epsilon^{2/5}$, $\eta^* = \zeta^* = \epsilon^{1/5}$ and, to lowest order,

$$\dot{h}^* - h^*\frac{\partial\phi}{\partial\tau} = -\frac{h^{*3}}{12}\frac{\partial}{\partial\xi}\left(\frac{1}{\phi^2}\frac{\partial\phi}{\partial\xi}\right) \tag{5.10}$$

where $h^* = h(t^*)$, $\dot{h}^* = \dot{h}(t^*)$. (When $\dot{h}^* = 0$, this equation can be transformed to the heat equation, but this situation is irrelevant to our current circumstances.)
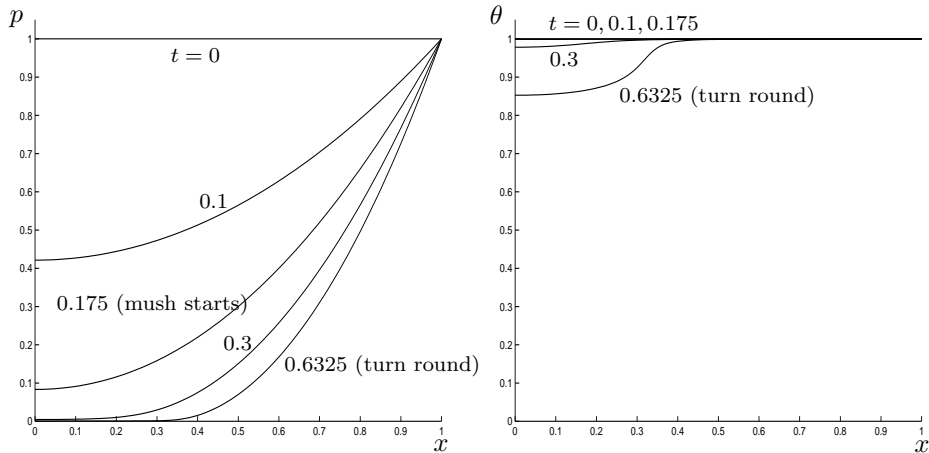
13

Figure 2: Expanding mush: p and θ versus x for the times shown.

The spatial matching conditions are that

$$\phi \sim \frac{\dot{h}^*}{h^*}\left(\tau + \sqrt{-\xi/k_-}\right) \qquad \text{as } \xi \to \infty,$$

this again being only affected by the earlier history of s, and

$$\phi \sim \frac{h^{*3}}{6\dot{h}^*}\xi^{-2} \qquad \text{as } \xi \to +\infty.$$

Moreover, the 'starting condition' for this turnover region comes from matching with (5.4)–(5.6), which is achieved if we demand that the solution of (5.10) tends, as $\tau \to -\infty$, to the 'stationary' solution of (5.4) with $V = 0$. Equally, the solution of (5.10) is expected to grow linearly in τ as $\tau \to \infty$, so that we can match with the 'stationary' solution $\theta = 1$ of (5.7)–(5.9). We will not expand here on the greater detail with which these matching procedures could be carried out; nor will we describe the analyses that can, in a similar spirit, be carried out for mush initiation and extinction.

5.4 Numerical experiments

It is relatively straightforward to solve equation (5.1) numerically in one space dimension; we used the NAG routine DO3PCF, with $h(t) = 1 + \frac{1}{2}t^2$, $\epsilon = 10^{-4}$, and for $0 < x < 1$ with a symmetry condition at $x = 0$ (so D is $-1 < x < 1$). Figures 2 and 3 show profiles of p and θ while the mush is first expanding and then contracting; note the difference in the behaviour of θ near the interface in the two cases. We also show contour plots of p and θ, in Figure 4; the initiation of the mush when $\epsilon = 0$ is at $t = 0.1744\ldots$ and the turn-round point $t = \sqrt{2/5}$, but even for our small value of ϵ the times at which these events happen for the regularised solution may be expected to differ noticeably from these values because, for example, $\epsilon^{1/3} \gg \epsilon$. Note the near-discontinuity at $t \approx 1.9$; this corresponds to the switch in the unregularised problem from the condition $p = 0$ on a contracting mush boundary to the symmetry condition $\partial p/\partial x = 0$ at $x = 0$ after the mush has vanished.

Lastly in Figure 5 we show three-dimensional plots of p and θ against x and t.

We have also carried out numerical computations for a simple two-dimensional configuration, in which D is a square. We aim to illustrate the reversibility of the unregularised model using
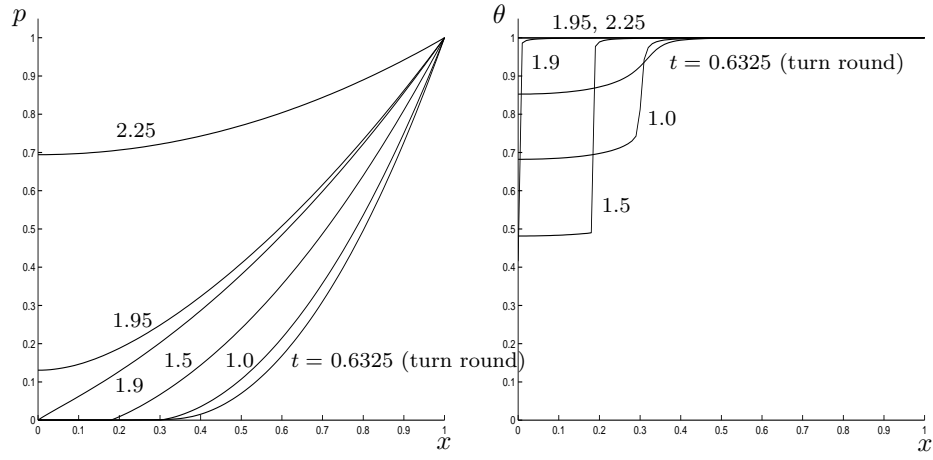
14

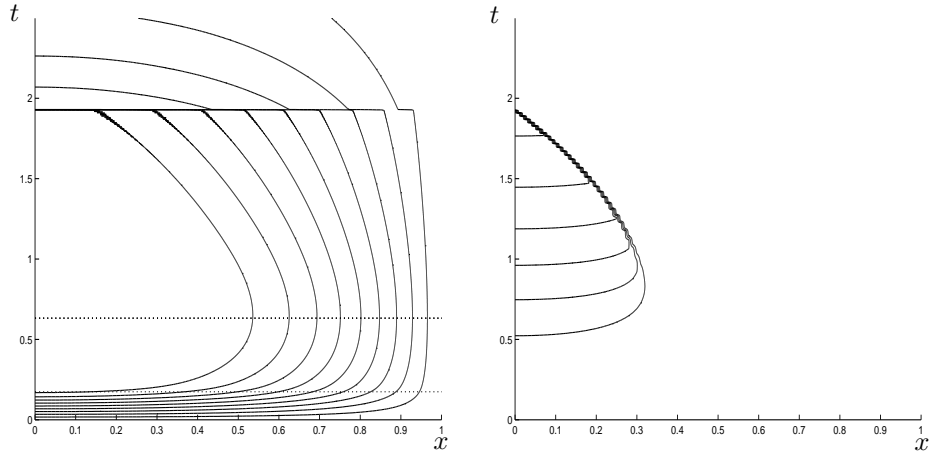Figure 3: Contracting mush: p and θ versus x for the times shown.

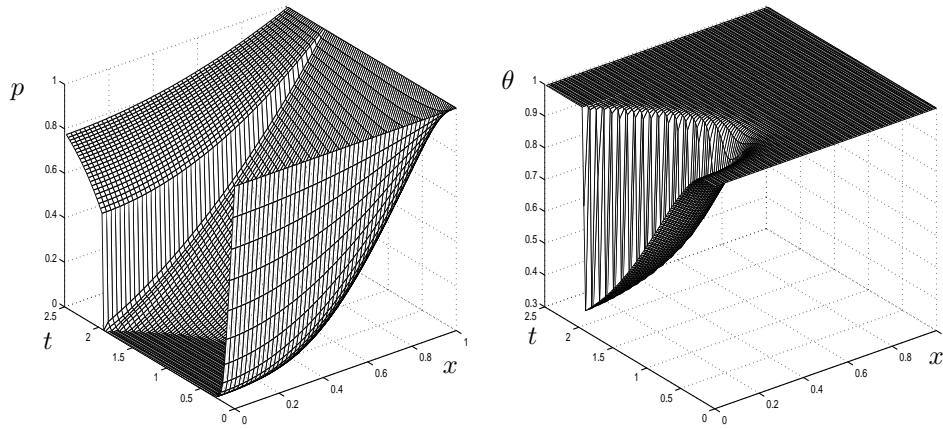Figure 4: Contour plots of p and θ (interval 0.1).
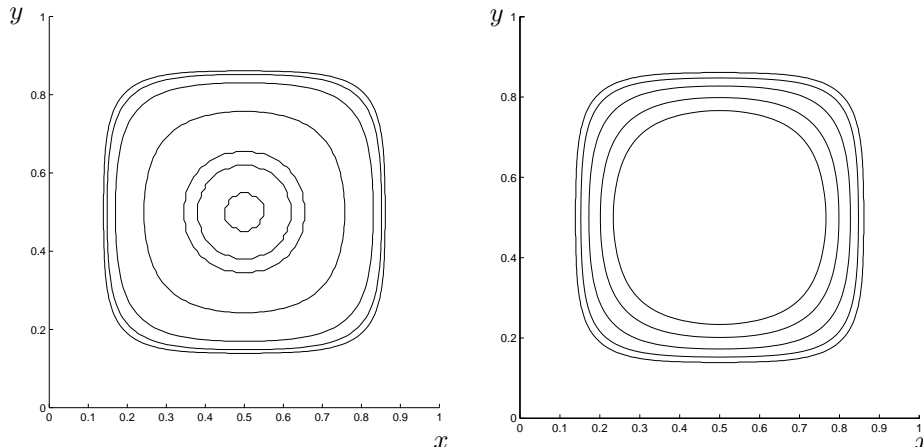

Figure 5: Mesh plots of p and θ.

15

Figure 6: Advancing (left) and receding (right) mush boundaries. In the advancing case, $\epsilon = 0.001$ and the level curve $\theta = 0.995$ is plotted at $t =$0.12, 0.22, 0.23, 0.3, 0.5, 0.7 and the turn-round time 1. The unevenness in the innermost curve is due to the mesh-size. The right-hand plot shows the contour $\theta = 0.995$, $t = 1$ from the left-hand plot ($\epsilon = 0.001$), together with the contour $\theta = 0.95$, $t = 1$, 1.5, 1.7 and 1.84 for $\epsilon = 0.01$.

the regularised version, and in doing so we identify the free boundary with a level curve of θ. A practical difficulty that arises is that the routine we used, D03RAF, cannot handle very small values of ϵ in the retreating mush phase, when gradients in θ of $O(1/\epsilon)$ occur; and if we use a larger value of ϵ, the difference between the regularised and unregularised solutions in the advancing mush phase becomes comparable to the solutions themselves, simply because the numerical value of w_M (defined in §4) is itself rather small, about 0.07 for a square of sides 1. As a compromise, and for illustrative purposes only, in Figure 6 we show advancing mush boundaries with $\epsilon = 0.001$ and receding boundaries with $\epsilon = 0.01$. In both cases, we take $F(t) = 36t(2 - t)$, for which the unregularised mush initiates at the time when $F = 1/w_M$, namely $t_i \approx 0.21$, and turns around at $t^* = 1$.

6 Conclusion

The relatively simple experiment that motivated this study has led to a free boundary model that can be most simply stated as the novel complementarity problem (2.13)–(2.17). From this model, it is not easy to discern the sequence of mush nucleation, expansion, turnover, contraction and extinction, but our identification of the close links between this model and that of classical Hele-Shaw free boundary flow provides an analytical explanation of some of these events for the special case of flat plates, as shown in §§3,4. Further support is provided by the regularisation proposed in §5 and the consequent numerical experiments of §6.

The fact that even the analysis of just the turnover region leads to such a complicated evolution problem for a nonlinear diffusion equation as (5.10) suggests that it will be difficult to devise a rigorous analysis of (5.1) that is uniformly valid in the limit when ϵ, the regularising parameter, tends to zero.

Acknowledgements

References

[1] Andreucci, D., Herrero, M.A. & Velazquez, J.J.L. (2001), *The classical one-phase Stefan problem: a catalog of interface behaviors*, Surv. Math. Ind. **9**, 247–337.

[2] Atthey, D.R. (1974) *A finite difference scheme for a class of melting problems*, J. Inst. Math. Appl. **13**, 353–366.

[3] Bayada, G., Boukrouche, M., & Talibi, M. El-A. (1995) *The transient Lubrication problem as a generalized Hele–Shaw type problem*, Journal for Analysis and its Applications **14**, 59–87.

[4] Bayada, G., Chambat, M., & El Aloui, M. (1990) *Variational formulation and finite element algorithms for cavitation problems*. ASME Journal of Tribology **112**, 398–403.

[5] Boedo, S. & Booker, J.F. (1995) *Cavitation in normal separation of square and circular plates.* ASME Journal of Tribology **117**, 406–410.

[6] Bonneau, D., Guines, D., Frère, J. & Toplosky, J. (1995) *EHD analysis, including structural inertia effects and mass-conserving cavitation model.* ASME Journal of Tribology **117**, 540–547.

[7] Coyne, J.C. & Elrod, H.G (1970) *Conditions for the rupture of a lubricating film: Part I, theoretical model.* J. Lub. Tech **92**, 451–456.

[8] Dowson, D., & Taylor, C.M. (1979) *Cavitation in bearings*, Ann. Rev. Fluid Mech. **11**, 35–66.

[9] Elliott, C.M. & Janovsky, V. (1981) *A variational inequality approach to Hele-Shaw flow with a moving boundary*, Proc. Roy. Soc. Edin. A – Math **88**, 93–107.

[10] Elliott, C.M. & Ockendon, J.R. (1982) *Weak and Variational Methods for Moving Boundary Problems.* Pitman Res. Notes in Mathematics **59**.

[11] Entov, V.M. & Etingof, P.I., (1991) *Bubble contraction in Hele-Shaw cells*, Quart. J. Mech. Appl. Math. **44**, 507–535.

[12] Fasano, A., Primicerio, M., Howison, S.D & Ockendon, J.R. (1990) *Some remarks on the regularisation of one-phase Stefan problems in one dimension.* Quart. Appl. Math. **48**, 153–168.

[13] Hays. D.F. & Feiten, J.B. (1964) *Cavitation between moving parallel plates*, in *Cavitation in Real Liquids*, ed. R. Davies, Elsevier New York.

[14] Kumar, A. & Booker , J.F. (1991) *A finite element cavitation algorithm*, Trans. ASME Tribology Division, **113**, 276–286.

[15] Lacey, A.A. & Herraiz, L.A. (2000) *Macroscopic models for melting derived from averaging microscopic Stefan problems. I: Simple geometries with kinetic undercooling or surface tension.* Europ. J. Appl. Math. **11**, 153–169.

[16] Lacey, A.A. & Tayler, A.B. (1983) *A mushy region in a Stefan problem*, I.M.A J. Appl. Math. **30**, 303–313.

[17] Murty, K.G. (1984) *Note on a Bard-type scheme for solving the complementarity problem.* Opsearch **11**, 123–130.

[18] Optasanu, V. & Bonneau, D. (2000) *Finite element mass-conserving cavitation algorithm in pure squeeze motion: validation/application to a connecting-rod small end bearing*, ASME J. Tribology **122**, 162–169.

[19] Rodrigues, A.N. (1970), *An analysis of cavitation in a circular squeeze film and correlation with experimental results*, Ph D thesis, Cornell University.

[20] Shelley MJ, Tian FR & Wlodarski K (1997) *Hele-Shaw flow and pattern formation in a time-dependent gap* Nonlinearity **10**, 1471–1495.

[21] Thamida SK, Takhistov PV & Chang HC (2001), *Fractal dewetting of a viscous adhesive film between separating parallel plates*, Phys. Fluids **13**, 2190–2200.